Table 1 Patient characteristics

Characteristic	Number	Rate (%)
Age (years)		
Range	50–81	
Median	66.5	
Sex		
Male	24	86
Female	4	14
Ascites		
Slight	1	3.5
Immediate	1	3.5
None	26	93
Bilirubin (mg/dL)		
<2	27	96
2–3	0	0
>3	1	4
Serum albumin (g/dL)		
>3.5	13	46.5
2.8–3.5	14	50
<2.8	1	3.5
PT (serum)		
>80%	8	29
60–80%	16	57
<60%	4	14
γ-GTP (IU/L)		
≤75	19	68
75–150	6	21
≥150	3	11
AFP status (μg/L)		
≤20	11	39
20–400	11	39
≥400	6	22
Child-Pugh classification		
A	16	57
B	12	43

AFP, α-fetoprotein; PT, prothrombin time; γ-GTP, gamma glutamine transpeptidase.

follows the natural flow of lymph. Portal lymph nodes include the hepatoduodenal ligament and common hepatic artery lymph nodes. Peri-pancreatic nodes consist of posterior pancreaticoduodenal and anterior pancreaticoduodenal lymph nodes. Paraaortic nodes are composed of celiac trunk and superior mesenteric artery as well as the middle colic artery lymph nodes.

Patient characteristics are listed in Table 1. The Karnofsky performance status score was greater than 90% in almost all patients. The median period from initial therapy for the primary tumors to EBRT for LNM was 34.6 months (3.2 months to 6.1 years). Whether or not patients received EBRT was a matter of physician preference because of the extent of the tumor, or at the discretion of the attending surgeon, and, ultimately, depended on the consent of the patient.

The Child-Pugh classification score was based on the levels of serum bilirubin, serum albumin, prothrombin time prolongation, presence or absence of ascites, and encephalopathy (Table 1).

Table 2 Characteristics of intrahepatic tumor

Characteristic	Number	Rate (%)
Intrahepatic tumor number		
Multiple (≥2 nodules)	8	67
Solitary	4	33
Maximal diameter (cm)		
≤2 cm	6	50
>2 cm	6	50
Vascular invasion		
(+)	1	8
(–)	11	92
TNM staging by LCSGJ		
I	2	17
II	3	25
III	6	50
IV	1	8
Previous therapy for intrahepatic tumors		
Resection	8	29
TAE	19	68
RFA	15	54
PEIT	5	18

LCSGJ, Liver Cancer Study Group of Japan; PEIT, percutaneous ethanol injection therapy; RFA, radiofrequency ablation; TAE, transcatheter arterial embolization.

Treatment plan

Patients received limited-field EBRT using a linear accelerator with 6-MV photon. The design and delivery of EBRT used a CT scan of the disease during the simulation process. The radiation portals encompassed the involved nodes with generous margins (2 cm) and were usually less than 100 cm^2. Parallel-opposed portals were frequently used. An isocentric technique was used and the source to axial distance (SAD) was 100 cm. The median tumor dose was 50 Gy (range 46–60 Gy) in daily 2.0-Gy fractions, five times a week. Twenty-two patients (79%) were given 50 Gy in 25 fractions. The total dose was less than or equal to 60 Gy in all patients. Two patients with ascites received the same dose (Table 4).

Follow-up

Enhanced CT scans between pre- and post-EBRT were compared. A complete response (CR) was defined as complete disappearance of all clinical and radiographic evidence of disease. A partial response (PR) required a 50% or greater reduction in the sum of the products of the longest diameter and its perpendicular of measurable lesions. Progressive disease was defined as an increase of ≥25% in the sum of the products of the longest diameter and its perpendicular, as compared with the lowest value recorded. Objective response (OR) was calculated for CR and PR.

For AFP positive patients, the serum AFP was also assayed in the first follow-up. AFP changes were compared with two investigations about 3 months apart, from pre-EBRT to 1 and half months after completion of EBRT. AFP decline required a value under 20 μg/L or a difference of 10% from a previous assay. Toxicity was evaluated according the Radiation Therapy Oncology Group criteria (version 2.0).[1]

Journal of Gastroenterology and Hepatology **22** (2007) 523–527 © 2006 The Authors
Journal compilation © 2007 Journal of Gastroenterology and Hepatology Foundation and Blackwell Publishing Asia Pty Ltd

Table 3 Characteristics of the target lymph node (LN) lesion

Characteristic	Number	Rate (%)
Location of the lesions (cumulative)		
Portal LN	10	36
PALN	12	43
Pre-pancreatic LN	2	7
Supra-clavicular LN	4	14
Peri-gastric LN	2	7
Peri-esophageal LN	2	7
Mediastinal LN	2	7
Axillary LN	1	3.6
Subphrenic LN	1	3.6
Hilar LN	1	3.6
Maximal diameter of LN		
≤2 cm	4	14
2–5 cm	19	68
≥5 cm	5	18
LN number		
Multiple	10	36
Solitary	18	64
Group		
Locoregional	17	61
Distant	11	39
Aim of RT		
Near-cure	21	75
Palliative	7	25
Other metastasis at the time of positive LN		
None	23	82
Lung	2	7
Bone	1	3.6
Systemic LN	1	3.6
Bone and lung and IVC	1	3.6

IVC, inferior vena cava; PALN, para-aortic lymph node; RT, radiotherapy.

Table 4 Radiotherapy method

	Number	Rate (%)
Total dose (Gy)		
46Gy/23Fr	1	4
50Gy/25Fr	23	82
60Gy/30fr	4	14
Treatment period (days)		
Range	21–63	
Median	35	
RT technique		
Three-dimensional conformal	8	28
Four-field box	15	54
AP-PA opposed fields	4	14
Wedge pair	1	4
Field length of *y*-axis direction (mm)		
<100	14	50
≥100	14	50
Field length of *x*-axis direction (mm)		
<100	20	71
≥100	8	29

AP, anteroposterior; Fr, fractionations; PA, posteroanterior.

Statistical methods

Statistical analyses were performed using StatView Dataset File version 5.0 J for Windows computers (North Carolina, USA). Overall survival (OS) was calculated from the first date of RT. Survival time was plotted using the Kaplan-Meier method. The Cox regression model was used to detect associations between survival and the following valuables: gender, serum AFP and γ-glutamyltransferase levels, intrahepatic tumor status (tumor size and number), LN status (location, number and size), and Child-Pugh classification.

Results

Follow-up

At the end of follow-up, 16 patients (57%) had died. Median follow-up time was 5.2 months (range 2–42 months).

Response and survival

In all patients, 18 (64%) and five (18%) patients achieved PR and CR, respectively (Table 5). In patients given EBRT for the near-cure intent (not palliative intent), the 1- and 2-year overall survival rates were 53% and 33%, respectively, and the median survival time (MST) was 13 months (Fig. 1).

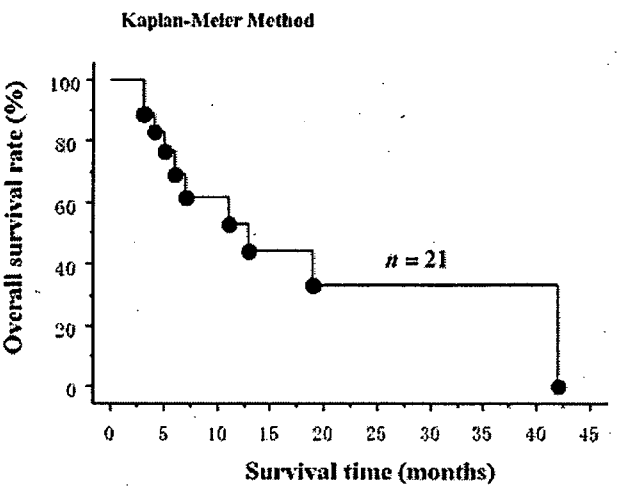

Figure 1 Overall survival curves for lymph node metastasis from HCC according to metastatic lesions.

Of the 28 HCC patients, 12 patients (43%) showed a significant decrease in their AFP levels, including three patients who returned to a normal level (≤20 μg/L). There were eight patients who showed AFP level increases or remained at the pretreatment level after EBRT.

Prognostic factors

The results of univariate and multivariate analyses of survival are listed in Table 6. Two factors appeared to be independently

Table 5 Univariate and multivariate analyses ($n = 21$) in relation to survival in patients given external beam radiation therapy (EBRT) for near-cure intent

Independent variable	Patients	Kaplan-Meier survival				Univariate analysis		Multivariate analysis	
	(*n*)	1-year (%)	2-year (%)	Median (M)	*P*-value	RR	*P*-value	RR	*P*-value
γ-GTP (IU/L)									
≤50	10	60.0	40.0	13.0	0.973	1	0.973	1	0.153
>50	11	48.0	32.0	11.0		1.02		34.28	
Sex									
Female	4	66.7	66.7	—	0.485	1	0.497	1	0.359
Male	17	51.4	27.4	13.0		2.04		0.029	
AFP (μg/L)									
≤30	8	57.1	38.1	19.0	0.705	1	0.707	1	0.417
>30	13	43.6	21.8	11.0		1.30		0.365	
Previous therapy for intrahepatic tumors									
Resection	6	30.0	0	6.0	0.047	1	0.065	1	0.060
Without resection	15	61.7	46.3	19.0		0.26		0.061	
Group									
Distant	6	80.0	40.0	19.0	0.401	1	0.411	1	0.384
Locoregional	15	40.3	26.9	11.0		1.96		0.15	
Child-Pugh classification									
A	12	30.5	30.5	7.0	0.352	1	0.363	1	0.057
B	9	87.5	32.8	19.0		0.52		0.014	
Maximal diameter of LN (cm)									
≤3.5	12	59.3	59.3	—	0.251	1	0.266	1	0.585
>3.5	9	46.7	15.6	11.0		2.21		2.74	
LN number									
Multiple	7	44.4	22.2	7.0	0.379	1	0.389	1	0.211
Solitary	14	55.9	37.2	19.0		0.56		0.058	
Response to EBRT									
OR	17	55.1	41.3	13.0	0.857	1	0.858	1	0.246
NC	4	50.0	25.0	11.0		1.14		0.11	

AFP, α-fetoprotein; LN, lymph node; M, months; NC, no change; OR, objective response; RR, relative risk.

Table 6 Side-effects of external beam radiotherapy

	Grade 1	Grade 2	Grade 3	Grade 4
Gastrointestinal				
Anorexia	11	1	0	0
Diarrhea	1	0	0	0
Gastro/duodenal ulcer	2	8	0	0
Dermatitis	3	2	0	0
Hepatic				
ALT (GPT)	6	7	0	0
Bilirubin	3	0	0	0
Bone marrow				
White blood cells	8	10	0	0
Platelets	12	5	4	0

ALT (GPT), alanine aminotransferase (glutamate pyruvate transaminase).

associated with the risk of death: (i) the Child-Pugh classification, with a worse prognosis with decreasing classification; and (ii) previous resection for intrahepatic tumors, with a worse prognosis.

Side-effects from external beam radiation therapy

No side-effects equal to or more than grade 3 such as loss of appetite and nausea, gastrointestinal bleeding or perforation induced by EBRT were seen. However, regarding bone marrow, thrombocytopenia of grade 3 was seen in four patients (14%) (Table 6).

Discussion

The predominant majority of HCC cases are restricted to the liver. Regional LNM are uncommon in HCC patients. The incidence of LN involvement in patients with HCC is between 1.6% and 5.9% during treatment,[2,3] but the incidence in autopsy cases has been as high as 30%.[4,5] During recent years an increasing incidence has been noted, possibly due to the interventional procedures carried out for patients with HCC, such as surgical resection, TAE, as well as PEIT.

Patients with LNM from HCC have a dire prognosis, even if radical resection is performed by experienced surgeons.[6–8] The survival in these patients treated with resection varied markedly

Journal of Gastroenterology and Hepatology 22 (2007) 523–527 © 2006 The Authors
Journal compilation © 2007 Journal of Gastroenterology and Hepatology Foundation and Blackwell Publishing Asia Pty Ltd

and ranged from 2 to 87 months (usually 3 months or less).[6–8] LN involvement is generally not the limiting factor in determining symptoms or survival, both of which relate more to hepatic parenchymal involvement or distant metastatic disease. The LN involvement is not rare and is documented by cited autopsy series. Therefore, in those series of unresectable cases LN status has generally been neglected. Also, TAE and PEIT were not suitable for these patients. EBRT was tried in these patients but was limited to only four HCC patients with abdominal LN involvement. These were described in two reports and one phase I clinical trial from China, appearing at an interval of 10 years. The former two papers showed CR in all, with improved longer survival. In the later paper, all of the 29 HCC patients with LN involvement who received EBRT achieved objective responses and their symptoms were completely relieved.[9] In our results, 64% and 18% of patients achieved PR and CR, respectively. In another study, Zeng *et al.* reported the radiosensitivity of HCC LN and concluded that LNM from HCC is sensitive to EBRT (50 Gy in 25 fractions).[10] Sixty-two patients with regional LNs received local limited EBRT (40–60 Gy in daily 2.0-Gy fractions). After EBRT, PR and CR were observed in 37% and 60% of patients, respectively, and the MST was 9.4 months.

The incidence of LNM in HCC patients is much higher in the autopsy series than in the clinical data.[2–5] This might mean LN involvement usually does not result in death of HCC patients. In our study, there was no significant difference in overall survival between one group with locoregional LNM and the other group with distant LNM ($P = 0.401$). This might suggest that RT for the locoregional LNM from HCC could not lead to improvement in survival.

As to the irradiation dose in our series, almost all patients were treated with 50 Gy (82%). Zeng *et al.*[9,10] recommended that the suitable irradiation dose should be limited to less than 56 Gy, because gastrointestinal bleeding incidence was much higher (33.3%) in patients given 56 Gy or higher. Additionally, they concluded that EBRT with 25 fractions of 2 Gy was an effective palliative treatment for patients with LNM from HCC presenting with good performance status.[10] Radiation complications consistently increased as the radiation dose increased, and gastrointestinal bleeding was a serious complication.[10] In our study, no gastrointestinal side-effect was observed. Our recommendation for a suitable radiation dose is 50 Gy.

In this study, AFP could not be used as a predictor in HCC patients with LNM treated with EBRT. This could be explained as lack of intrahepatic tumor and/or distant metastasis control, which resulted in treatment failure. Although LNM from HCC is sensitive to EBRT, the intent of EBRT should be limited to palliation. EBRT is useful in treatment with 50 Gy in 25 fractions for these patients.

References

1 Trotti A, Byhardt R, Stetz J *et al.* Common Toxicity Criteria (version 2.0): an improved reference for grading the acute effects of cancer treatment—impact on radiotherapy. *Int. J. Radiat. Oncol. Biol. Phys.* 2000; 47: 13–47.

2 Ueno N, Kanamaru T, Kawaguchi K *et al.* A hepatocellular carcinoma with lymph node metastasis and invasion into the gallbladder: preoperative difficulty ruling out a gallbladder carcinoma. *Oncol. Rep.* 2001; 8: 331–5.

3 Kubicka S, Rudolph KL, Hanke M *et al.* Hepatocellular carcinoma in Germany: a retrospective epidemiological study from a low-endemic area. *Liver* 2000; 20: 312–18.

4 Watanabe J, Nakashima O, Kojiro M. Clinicopathologic study on lymph node metastasis of hepatocellular carcinoma: a retrospective study of 660 consecutive autopsy cases. *Jpn J. Clin. Oncol.* 1994; 24: 37–41.

5 Yuki K, Hirohashi S, Sakamoto M *et al.* Growth and spread of hepatocellular carcinoma. A review of 240 consecutive autopsy cases. *Cancer* 1990; 66: 2174–9.

6 Uenishi T, Hirohashi K, Shuto T *et al.* The clinical significance of lymph node metastases in patients undergoing surgery for hepatocellular carcinoma. *Surg. Today* 2000; 30: 892–5.

7 Uenishi T, Hirohashi K, Tanaka H *et al.* A surgically treated case of hepatocellular carcinoma with extensive lymph node metastases. *Hepatogastroenterology* 2000; 47: 1714–16.

8 Toyoda H, Fukuda Y, Koyama Y *et al.* Case report: multiple systemic lymph node metastases from a small hepatocellular carcinoma. *J. Gastroenterol. Hepatol.* 1996; 11: 959–62.

9 Zeng ZC, Tang ZY, Yang BH *et al.* Radiation therapy for the locoregional lymph node metastases from hepatocellular carcinoma, phase I clinical trial. *Hepatogastroenterology* 2004; 51: 201–7.

10 Zeng ZC, Tang ZY, Fan J *et al.* Consideration of radiotherapy for lymph node metastases in patients with HCC: retrospective analysis for prognostic factors from 125 patients. *Int. J Radiat. Oncol. Biol. Phys.* 2005; 63: 1067–76.

A Rod Matrix Compensator for Small-Field Intensity Modulated Radiation Therapy: A Preliminary Phantom Study

Keiichi Nakagawa, Kiyoshi Yoda*, Yoshitaka Masutani, Katsutake Sasaki, and Kuni Ohtomo

***Abstract*—A compensator made of a tungsten-based rod matrix has been proposed for small-field intensity modulated radiation therapy. The compensator was attached to a 6 MV linac gantry head. The proposed compensator could modulate the X-ray intensity with a step of 10% and a minimum transmission of 2.5%.**

***Index Terms*—Compensator, IMRT, intensity modulation, radiotherapy.**

I. Introduction

The concept of inverse planning and intensity modulated radiation therapy (IMRT) was proposed by Brahme [1]. The inverse planning is a mathematical optimization procedure in order to deliver sufficiently high dose to a tumor while minimizing dose in healthy organs located adjacent to the tumor. Using the resulting inverse planning solution, the IMRT can be physically realized by two different ways: a dynamic way and a static way.

The dynamic technique utilizes motor-driven multileaf collimators (MLCs) comprising narrow metal bars (leaves) aligned parallel to each other. The irradiated X-ray intensity can be spatially modulated by moving MLCs during X-ray beam delivery. This MLC-based IMRT has been widely accepted because intensity modulation can be automatically planned by using a treatment planning computer. An additional advantage that has been recently reported is a tracking capability for a moving target [2], [3]. A disadvantage of the MLC-based IMRT is that it requires much longer delivery time thereby increasing the chance of organ movements during treatment.

Meanwhile, compensators for high energy X-ray treatment were proposed long time ago [4], and Brahme suggested this as a means for intensity modulation [1]. Several research groups have employed this compensator-based IMRT [5]–[10]. Although the static compensator simplifies the treatment delivery with reduced beam-on time, technologists need to enter the treatment room and exchange compensators port by port. Other disadvantages of compensator-based IMRT are the fabrication time as well as constantly produced compensator wastes.

Recently, dosimetrically less precise compensators for quick fabrication have been proposed [11]–[13], where the compensator can be automatically exchanged. However, these fabrication methods required complicated machines. We have developed a rod matrix compensator that does not require an expensive fabrication machine. The proposed compensator can be manually fabricated within 10 min, and it can be reused without producing wastes.

II. Methods and Materials

Fig. 1(a) shows a photograph of 11 different compensator rods each comprising tungsten compound for X-ray intensity attenuation and wood support for keeping the total rod length to 50 mm. The cross section has a dimension of 5 mm × 5 mm. The tungsten compound has a density of 19.3 g/cm^3 (Heavy Metal, Sumitomo Electric) while the wood support has a density of 0.35 g/cm^3. The tungsten compound and the wood support were bonded by adhesive resin, and each rod has a specific identification (ID) number printed on a surface.

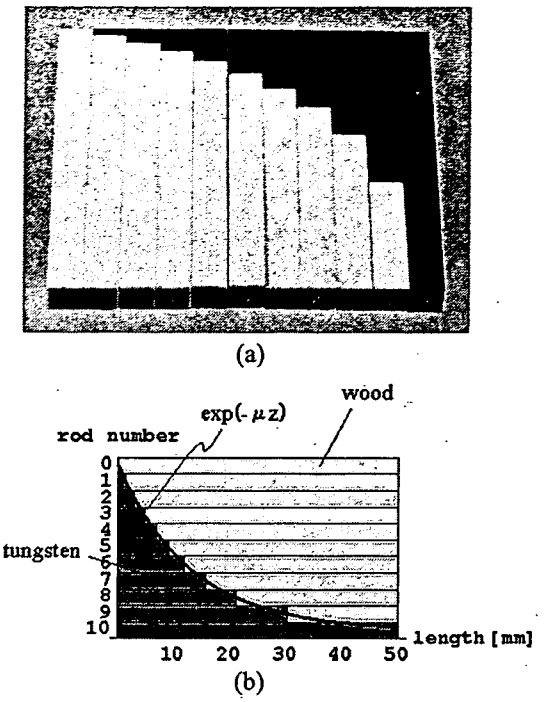

Fig. 1. (a) A photograph of the compensator rods each comprising tungsten compound for intensity modulation and wood support for keeping the total rod length to 50 mm. (b) The length of the tungsten compound was optimized to provide a constant incremental step of 10% attenuation.

Fig. 1(b) shows a mathematical diagram that describes how to determine the length of the tungsten compound for providing a constant incremental step of 10% X-ray attenuation. Each tungsten length is determined by an exponential function $exp(-\mu z)$ where μ is a linear attenuation coefficient of the tungsten compound for a given X-ray energy and z is the length of the tungsten compound. The attenuation caused by the wood support is ignored.

Fig. 2 shows a photograph of the compensator fabrication unit including a metal wall having a foldable portion, a rod matrix piled up inside the wall, a base stand, and a 5 mm thick acrylic base plate that interfaces between the metal wall and the base plate. To support the rod matrix at the bottom, a transparent acrylic plate (1 mm thickness) was inserted, in parallel to the acrylic base plate, into the groove provided near the bottom of the metal wall. Each rod was manually piled up to make an 11 by 11 rod matrix. The foldable part of the metal wall remained open during the piling up process. Because each rod has an ID number corresponding to a particular attenuation level, it was straightforward to pile up the rods according to a given intensity map. After piling up 11 by 11 rods, another 1 mm thick transparent acrylic cover plate was inserted into another groove provided near the top of the metal wall. Finally, the open portion of the metal wall was folded and locked firmly to immobilize the rod matrix.

Fig. 3 depicts a photograph of the resulting compensator attached to the gantry head of a 6 MV Mitsubishi C-arm linac, CRS-6000. For preliminary testing purpose, the distance between the X-ray source and

Manuscript received February 22, 2006; revised October 14, 2006. *Asterisk indicates corresponding author.*

K. Nakagawa, Y. Masutani, K. Sasaki, and K. Ohtomo are with the Department of Radiology, Faculty of Medicine, University of Tokyo Hospital, Tokyo 113-8655 Japan (e-mail: nakagawa-rad@umin.ac.jp).

*K. Yoda is with Elekta K. K., 6-1-9 Isogami-dori, Chuo-ku, Kobe 651-0086 Japan (e-mail: kyo@elekta.co.jp).

Digital Object Identifier 10.1109/TBME.2007.893490

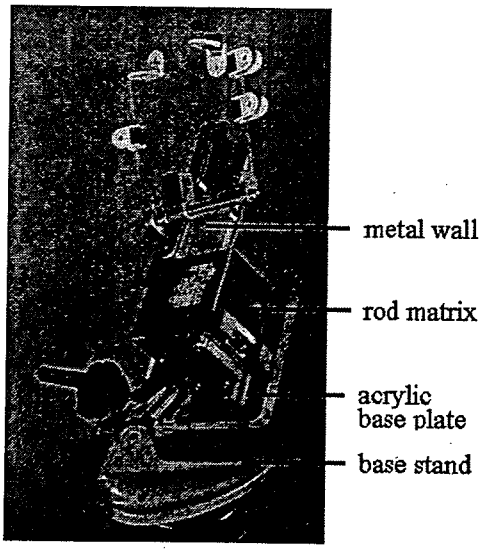

Fig. 2. A photograph of the compensator assembling unit. Each compensator rod was manually piled up to make 11 by 11 rod matrix.

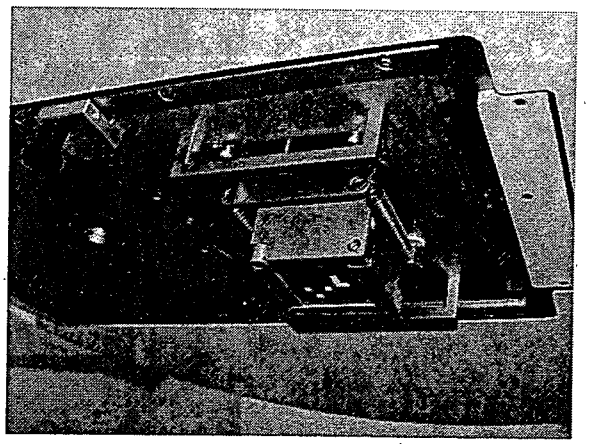

Fig. 3. A photograph of the assembled compensator attached to the gantry head.

the bottom plane of the compensator rods was 530.5 mm. The projected field size of the 11 by 11 rod matrix on the isocenter (center of gantry rotation) plane was approximately 104 mm × 104 mm. Although most of previous compensators required the MLC to shield outside the tumor target region, the proposed compensator would require only block collimators to avoid radiation on and outside the compensator metal wall because the X-ray transmission through the 50 mm tungsten rod was considered sufficiently small. In order to minimize the inter-rod leakage on the central axis, the rods were firmly compressed by the metal wall and were aligned to a half-offset position with respect to the central axis. 5000 MU (Monitor Unit) was delivered to an X-ray film (EDR2, Kodak) through an 11 by 11 rod matrix having a tungsten thickness of 50 mm to evaluate the inter-rod leakage and the transmission.

Subsequently, tungsten compound plates (Heavy Metal, Sumitomo Electric) each having a thickness of 5 mm were piled up to provide 0, 5, 15, 25, 35, 50 mm thickness for determining the X-ray linear attenuation coefficient. The material property of the tungsten rod and the tungsten plate was identical. The X-ray transmission was measured by a Farmer type ion chamber (0.6 cm^3, PTW TN30013) as a function of the thickness of the tungsten compound. The ion chamber was placed

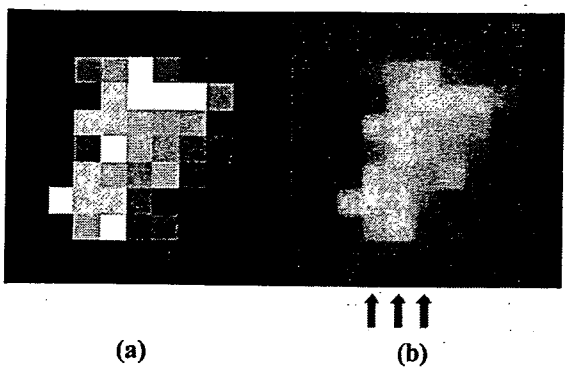

Fig. 4. (a) Simulated intensity map based on a simple exponential model. (b) Dose profile read by the film scanner.

at the depth of 100 mm solid water phantom, which coincided with the isocenter position. Another 100 mm solid water phantom was placed below the isocenter. A tray factor, when no rods were placed between the two 1-mm-thick acrylic plates in the compensator enclosure, was also measured. The calculation of the linear attenuation coefficient was repeated with three different field sizes of 30 mm × 30 mm, 50 mm × 50 mm, and 70 mm × 70 mm. The resulting attenuation coefficients were plotted as a function of the side length of the square field, and the linear attenuation coefficient without scattering effect was obtained by extrapolating the plot to field size zero.

After determining the linear attenuation coefficient of the tungsten compound for our 6 MV linac, each tungsten rod length was calculated according to the rule shown in Fig. 1(b). Then, a compensator was constructed to test intensity modulation capability. Another EDR2 film was positioned perpendicular to the beam axis on an isocenter plane with two 100 mm solid water phantoms above and below the film. After delivering 300 MU, the intensity modulated dose profiles on the film were measured by a film scanner (R-TECH, DD system) and compared to the intensity map calculated by the measured linear attenuation coefficient and the simple exponential model [5].

III. Results

Based on the measured tray factor of 0.979 and TMR (Tissue Maximum Ratio) of 0.7913 at 100-mm depth for a field size of 100 mm × 100 mm, the transmission through the 50 mm tungsten rod matrix was approximately 2.5% and the maximum leakage between rods was approximately 2.7% according to the film readings.

The semi-log plot of X-ray transmission was linear up to 50 mm tungsten length for each of the three different field sizes, and a linear attenuation coefficient of 0.0763 mm^{-1} was obtained. The lengths of the tungsten compound were determined as follows: 1.38, 2.92, 4.67, 6.69, 9.08, 12.01, 15.78, 21.09, 30.18, and 50.0 mm. Fig. 4(a) shows a simulated intensity map calculated from the exponential attenuation model with the measured linear attenuation coefficient. Fig. 4(b) shows measured dose distribution using the film. The vertical arrows indicate the scanning lines, and the scanned results are shown in the next figure.

Fig. 5(a)–(c) demonstrates relative dose distribution read by the film scanner. The step patterns show calculated intensity profiles using the measured linear attenuation coefficient and the exponential attenuation model.

IV. Discussion

Unlike the previous cubic-block-based compensator having a fixed height [13], the proposed rod matrix compensator can provide a con-

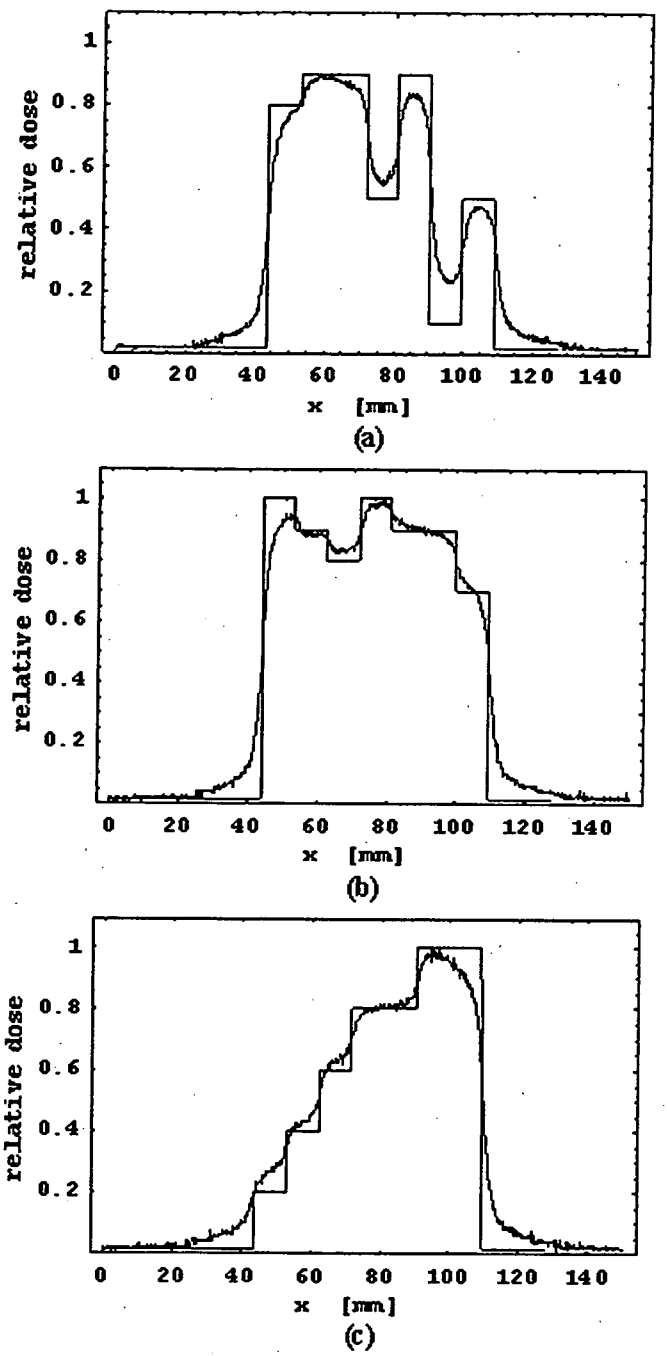

Fig. 5. (a)–(c) Relative dose distribution read by the film scanner. The scanned line positions correspond to the three vertical arrows in Fig. 4(b) from left to right in order. The step patterns show calculated intensity profiles using the measured linear attenuation coefficient and the exponential attenuation model.

stant incremental intensity step of 10% by optimizing each length of the tungsten portion. Another advantage of the rod matrix compensator is that a multileaf collimator is not required to shield outside the target region. This means that the rod matrix compensator allows a linac without MLC to perform IMRT. The previous cubic-block-based compensator employed a tungsten-dominant resin having a density of as low as 12 g/cm^3; and therefore, piled-up blocks of 50-mm height led to 10% transmission [13].

In Fig. 5(a) –(c), we see reasonable correspondence between dose measurement and intensity calculation. It is well known that an X-ray film containing silver has a significantly higher sensitivity at an X-ray energy below 100 keV due to photo electric effect. In addition, the beam energy is quickly degraded at the time of lateral scattering [14]. Consequently, the lateral scattering in the water phantom would be the cause of the significant discrepancies at the two low dose regions near the center of Fig. 5(a). A very similar result was also demonstrated and discussed in a reference [15] that may also support this speculation.

The proposed compensator can be used with a rotating mount means [12]. This combination minimizes human labor during treatment because several compensators can be exchanged automatically. A major disadvantage of the proposed compensator is that the maximum field size is limited to 11 cm × 11 cm when the compensator is placed at a distance of 50 cm from the source. However the proposed compensators are considered to be an effective tool for a small tumor treatment because delivery time is comparable to conventional open beam treatment. It should be noted that a small tumor needs to be positioned more accurately than a large tumor and more time-consuming MLC-based IMRT would increase the chance of organ movements during treatment.

In the meantime, Shirato reported that their fluoroscopic breathing-gated procedure led to excessive kV dose if used with MLC-based IMRT that requires longer treatment time [16]. The prolonged dose delivery may also have an undesirable radiobiological impact on IMRT treatment outcome [17]. It is, therefore, expected that these issues can be effectively solved by using a compensator-based IMRT. Compensator-based IMRT dose calculation using Pinnacle treatment planning system (Philips/ADAC) is under commissioning phase, and the three-dimensional dose verification with the proposed compensator will be reported in the near future.

REFERENCES

[1] A. Brahme, "Optimization of stationary and moving beam radiation therapy techniques," *Radiother. Oncol.*, vol. 12, pp. 129–140, 1988.
[2] P. J. Keall, H. Cattell, D. Pokhrel, S. Dieterich, K. H. Wong, M. J. Murphy, S. S. Vedam, K. Wijesooriya, and R. Mohan, "Geometric accuracy of a real-time target tracking system with dynamic multileaf collimator tracking system," *Int. J. Radiat. Oncol. Biol. Phys.*, vol. 65, pp. 1579–1584, 2006.
[3] S. Webb, "Motion effects in (intensity modulated) radiation therapy: A review," *Phys. Med. Biol.*, vol. 51, pp. R403–R425, 2006.
[4] F. Ellis, E. J. Hall, and R. Oliver, "A compensator for variations in tissue thickness for high energy beams," *Br. J. Radiol.*, vol. 32, pp. 421–422, 1959.
[5] A. Djordjevich, D. J. Bonham, E. M. A. Hussein, J. W. Andrew, and M. E. Hale, "Optimal design of radiation compensators," *Med. Phys.*, vol. 17, pp. 397–404, 1990.
[6] J. Stein, K. Hartwig, S. Levegrun, G. Zhang, K. Preiser, G. Rhein, J. Debus, and T. Bortfeld, "Intensity-modulated treatments: Compensators vs. multileaf modulation," in *Proc. XIIth ICCR*, Salt Lake City, UT, May 1997, pp. 338–341.
[7] S. B. Jiang and K. M. Ayyangar, "On compensator design for photon beam intensity-modulated conformal therapy," *Med. Phys.*, vol. 25, pp. 668–675, 1998.
[8] S. X. Chang, K. M. Deschesne, T. J. Cullip, S. A. Parker, and J. Earnhart, "A comparison of different intensity modulation treatment techniques for tangential breast irradiation," *Int. J. Radiat. Oncol. Biol. Phys.*, vol. 45, pp. 1305–1314, 1999.
[9] S. X. Chang, T. J. Cullip, and K. M. Deschesne, "Intensity modulation delivery techniques: Step & shoot MLC auto-sequence versus the use of a modulator," *Med. Phys.*, vol. 27, pp. 948–959, 2000.
[10] S. X. Chang, T. J. Cullip, K. M. Deschesne, E. P. Miller, and J. G. Rosenman, "Compensators: An alternative IMRT delivery technique," *J. Appl. Clin. Med. Phys.*, vol. 5, pp. 15–36, 2004.
[11] T. Xu, P. M. Shikhaliev, M. Al-Ghazi, and S. Molloi, "Reshapable physical modulator for intensity modulated radiation therapy," *Med. Phys.*, vol. 29, pp. 2222–2229, 2002.

[12] K. Yoda and Y. Aoki, "A multiportal compensator system for IMRT delivery," *Med. Phys.*, vol. 30, pp. 880–886, 2003.
[13] K. Nakagawa, N. Fukuhara, and H. Kawakami, "A packed building-block compensator (TETRIS-RT) and feasibility for IMRT delivery," *Med. Phys.*, vol. 32, pp. 2231–2235, 2005.
[14] S. E. Burch, K. J. Kearfott, J. H. Trueblood, W. C. Sheils, J. I. Yeo, and C. K. C. Wang, "A new approach to film dosimetry for high energy photon beams: Lateral scatter filtering," *Med. Phys.*, vol. 24, pp. 775–783, 1997.
[15] Å. Palm, A. S. Kirov, and T. LoSasso, "Predicting energy response of radiographic film in a 6 MV X-ray beam using Monte Carlo calculated fluence spectra and absorbed dose," *Med. Phys.*, vol. 31, pp. 3168–3178, 2004.
[16] H. Shirato, M. Oita, K. Fujita, Y. Watanabe, and K. Miyasaka, "Feasibility of synchronization of real-time tumor-tracking radiotherapy and intensity-modulated radiotherapy from viewpoint of excessive dose from fluoroscopy," *Int. J. Radiat. Oncol. Biol. Phys.*, vol. 60, pp. 335–341, 2004.
[17] J. Z. Wang, X. A. Li, W. D. D'Souza, and R. D. Stewart, "Impact of prolonged fraction delivery times on tumor control: A note of caution for intensity-modulated radiation therapy (IMRT)," *Int. J. Radiat. Oncol. Biol. Phys.*, vol. 57, pp. 543–552, 2003.

Radiation Oncology

BioMed Central

Research

Open Access

Exceptionally high incidence of symptomatic grade 2–5 radiation pneumonitis after stereotactic radiation therapy for lung tumors

Hideomi Yamashita*, Keiichi Nakagawa, Naoki Nakamura, Hiroki Koyanagi, Masao Tago, Hiroshi Igaki, Kenshiro Shiraishi, Nakashi Sasano and Kuni Ohtomo

Address: Department of Radiology, University of Tokyo Hospital, Japan

Email: Hideomi Yamashita* - yamachan07291973@yahoo.co.jp; Keiichi Nakagawa - nakagawa-rad@umin.ac.jp; Naoki Nakamura - nnakamur-tky@umin.ac.jp; Hiroki Koyanagi - t34059@yahoo.co.jp; Masao Tago - tago-rad@h.u-tokyo.ac.jp; Hiroshi Igaki - igaki-tky@umin.ac.jp; Kenshiro Shiraishi - kshiraishi-tky@umin.ac.jp; Nakashi Sasano - sasanon-tky@umin.ac.jp; Kuni Ohtomo - kotomo-tky@umin.ac.jp

* Corresponding author

Published: 7 June 2007

Radiation Oncology 2007, 2:21 doi:10.1186/1748-717X-2-21

Received: 17 April 2007

Accepted: 7 June 2007

This article is available from: http://www.ro-journal.com/content/2/1/21

Abstract

Background: To determine the usefulness of dose volume histogram (DVH) factors for predicting the occurrence of radiation pneumonitis (RP) after application of stereotactic radiation therapy (SRT) for lung tumors, DVH factors were measured before irradiation.

Methods: From May 2004 to April 2006, 25 patients were treated with SRT at the University of Tokyo Hospital. Eighteen patients had primary lung cancer and seven had metastatic lung cancer. SRT was given in 6–7 fields with an isocenter dose of 48 Gy in four fractions over 5–8 days by linear accelerator.

Results: Seven of the 25 patients suffered from RP of symptomatic grade 2–5 according to the NCI-CTC version 3.0. The overall incidence rate of RP grade2 or more was 29% at 18 months after completing SRT and three patients died from RP. RP occurred at significantly increased frequencies in patients with higher conformity index (CI) ($p = 0.0394$). Mean lung dose (MLD) showed a significant correlation with V_5–V_{20} (irradiated lung volume) ($p < 0.001$) but showed no correlation with CI. RP did not statistically correlate with MLD. MLD had the strongest correlation with V_5.

Conclusion: Even in SRT, when large volumes of lung parenchyma are irradiated to such high doses as the minimum dose within planning target volume, the incidence of lung toxicity can become high.

1. Background

Since 1990, stereotactic radiotherapy (SRT) has been widely available for the treatment of intracranial lesions. Recently, the use of SRT has gradually been expanded to include the treatment of extra-cranial lesions. In particular, SRT has been demonstrated as a safe and effective modality in the treatment of primary and metastatic lung tumors [1]. Initial clinical results were favorable, and local control rates around 90% have been reported [1-9]. Since May 2004, we have employed SRT for body trunk tumors using a simple body cast system at the University of Tokyo Hospital.

Regarding normal tissue, the use of a single dose rather than a conventional fractionated dose may increase the risk of complications. However, few cases with severe toxicity have been reported [10].

A few patients undergoing high-dose SRT suffered from RP, which was treated by administration of steroids. The percentage of total lung volume receiving greater than or equal to 20 Gy (V_{20}) was reported to be a useful factor for RP in conventional fractions [11]. The useful dose volume histogram (DVH) factors were examined for predicting the occurrence of RP after SRT for lung tumors.

2. Methods

2.1. Patients and tumor characteristics

From May 2004 to April 2006, 25 patients were treated with SRT using a stereotactic body cast system using a custom bed and low temperature thermoplastic material RAYCAST® (ORFIT Industries, Wijnegem, Belgium) at the University of Tokyo Hospital. All patients enrolled in this study satisfied the following eligibility criteria: 1) solitary or double lung tumors; 2) tumor diameter < 40 mm; 3) no evidence of regional lymph node metastasis; 4) Karnofsky performance status scale ≧ 80% ; and 5) tumor not located adjacent to major bronchus, esophagus, spinal cord, or great vessels. Of the 25 patients, 16 had primary lung cancer, seven had metastatic lung cancer, and two had recurrent lung cancer. Ten patients were inoperable because of coexisting disease and one refused surgery. The primary lung cancers were staged as T1N0M0 in 15 and T2N0M0 in one. The primary sites of the metastases were the rectum, kidney, and ampulla of Vater in one each. A complete history was taken from all patients, and each received a physical examination, blood test, chest computed tomography (CT) scan, and whole-body positron emission tomography (PET) scan using FDG before treatment. Patient characteristics are summarized in Table 1.

In our clinical cases, five could not be histologically confirmed because the patients could not tolerate CT-guided biopsy and transbronchoscopic lung biopsy (TBLB). In these patients, the tumor diagnosis was confirmed clinically by a growing tumor on repeated CT scans and by exclusion of another primary tumor by clinical staging. None of the patients received concurrent chemotherapy with SRT. Additionally, no chemotherapy, which might affect the RP rates, was given prior to or immediately after SRT (until two months).

2.2. Planning procedure and treatment

The patient was positioned in a supine position on a custom bed. A body cast was made to broadly cover the chest to the abdomen during shallow respiration, and attached rigidly to the sidewall of the base plate.

The CT slice thickness and pitch were 1 mm each in the area of the tumor, and 5 mm each in the other areas. Each CT slice was scanned with an acquisition time of four seconds to include the whole phase of one respiratory cycle. A series of CT images, therefore, included the tumor and its respiratory motion. The axial CT images were transferred to a 3-dimension RT treatment-planning machine (Pinnacle^3, New Version 7.4i, Philips). Treatment planning was performed using the 3D RTP machine. The target volume corresponded to the internal target volume (ITV) in Japan Clinical Oncology Group (JCOG) 0403 phase II protocol [12]. The CT images already included the internal motion because long scan time (four seconds) CT under free breathing (what is called, "slow" CT scan) was used [13,14]. Spicula formation and pleural indentation were included within the ITV. The setup margin (SM) between ITV and the planning target volume (PTV) was 5 mm in all directions. Additionally, there was additional 5 mm leaf margin to PTV, according to JCOG0403 protocol, in order to make the dose distribution within the PTV more homogeneous. Two to 4 multi-leaf-collimator (MLC)-shaped non-coplanar static ports of 6-MV X-rays were selected to decrease mean lung dose (MLD), V_{20}, and V_{15} to below 18.0 Gy, 20%, and 25%, respectively, according to JCOG0403 protocol, although such numbers as V20 < 20% and V15 < 25% were valid for fractionation doses of about 2 Gy. We used no pairs of parallel opposing fields. The target reference point dose was defined at the isocenter of the beam. The collapsed cone (CC) convolution method was used as the dose calculation, in which the range of Compton electrons was better taken into account. In short, the convolution describes radiation interactions including charged particle transport, and calculates dose derived from CT density and patient set up information. The collapsed cone convolution method uses an analytical kernel represented by a set of cones, the energy deposited in which is collapsed onto a line (hence the name). The method is used to reduce computation time. In practice, the method utilizes a lattice of rays, such that each voxel is crossed by one ray corresponding to each cone axis. The primary beams were calculated heterogeneously and the scatter beams homogeneously as dose computation parameters. SRT was given with a central dose of 48 Gy in four fractions over 5–8 days in 6–7 fields by linear accelerator (SRL6000, Mitsubishi Electric Co., Tokyo) excluding two cases. Two patients (case no. 14 and 19) received 48 Gy in more than 4 fractionations (6 and 8 fractionations, respectively) (Table 2) since the tumor located in the hilar (central) region. As to the peripheral dose of the PTV, we checked that 95% PTV volumes coverage dose (D95) was over 90% of the central dose. CT verification of the target isocenter was performed to ensure the correct target position and sufficient reproducibility of suppressing breathing mobility before each treatment session.

Table 1: Details of patient characteristics

No.	Age	Sex	Primary site	Subject	Histology of target lesion	Chronic Lung Disorder	Inoperable reason	K-PS (%)	s KL (U/ml)	s SP-D (ng/ml)	VC (L)	FEV1.0 (L)
1	75	M	lung	primary	Adenoca	No	reject	90	wnl	wnl	4.07	2.81
2	83	M	lung	primary	Unknown	No	TAA/IHD	90	wnl	wnl	NA	NA
3	50	F	rectum	metastasis	Adenoca	post lobectomy	rectal ca.	90	wnl	wnl	3.40	2.66
4	77	M	lung	recurrence	SCLC	emphysema	SCLC-ED	90	wnl	wnl	NA	NA
5	75	M	lung	primary	Adenoca	No	nephrotic syndrome	80	wnl	wnl	NA	NA
6	60	M	lung	metastasis	Adenoca	post lobectomy	metastasis	90	743	wnl	2.61	0.59
7	79	M	lung	primary	SqCC	emphysema	colon ca./prostate ca.	90	wnl	wnl	1.75	1.26
8	79	M	ampulla of Vater	metastasis	Unknown	No	metastasis	80	wnl	wnl	NA	NA
9	69	M	lung	recurrence	Aenoca	post partial resection	recurrence	90	wnl	wnl	NA	NA
10	84	M	lung	primary	SqCC	No	TAA	70	wnl	wnl	1.74	0.85
11	81	M	lung	primary	Adenoca	No	M valve replacement	80	wnl	wnl	3.19	2.30
12	82	M	lung	primary	SqCC	No	prostate ca.	80	wn	wn	2.50	1.75
13	72	M	lung	metastasis	SqCC	No	metastasis	80	950	NA	2.76	2.13
14	80	M	lung	primary	Unknown	emphysema	HCC/colon ca.	80	NA	NA	NA	NA
15	80	M	kidney	metastasis	Unknown	No	Renal cell carcinoma	80	529	wnl	NA	NA
16	60	M	lung	metastasis	Carcinoma	IP	metastasis	80	852	NA	4.01	3.24
17	77	M	lung	primary	NSCLC	IP	IP	80	1590	NA	3.05	1.59
18	68	M	lung	primary	Adenoca	COPD	COPD	70	NA	NA	NA	NA
19	79	M	lung	primary	SqCC	emphysema	AAA	90	520	NA	NA	NA
20	64	F	lung	primary	Adenoca	No	CRF/IHD	90	wnl	wnl	2.04	1.56
21	76	F	lung	primary	SCLC	No	bladder ca./breast ca.	90	wnl	wnl	2.17	1.59
22	77	M	lung	primary	SqCC	No	diabetic nephropathy	80	wnl	wnl	NA	NA
23	78	M	lung	primary	NSCLC	IP	IP	80	wnl	127	NA	NA
24	62	M	colon	metastasis	Unknown	No	colon ca.	90	wnl	wnl	3.69	2.87
25	78	F	lung	primary	Carcinoma	IP/post lobectomy	post lobectomy	90	wnl	wnl	1.54	0.99
									(0–500)	(0–110)		

AAA: abdominal aortic aneurysm, Adenoca: adenocarcinoma, ca.: cancer, COPD: chronic obstructive pulmonary disea
ED: extended disease, FEV: forced expiratory volume, HCC: hepatocellular carcinoma, IHD: ischemic heart disease, IP?
K-PS: karnofsky performance status scale, M valve: mitral valve, NA: not available, s: serum, TAA: thoracic aortic ane
RP: radiation pneumonitis, SCLC:small cell lung cancer, SP-D: surfactant protein-D, SqCC: squamous cell carcinoma,

2.3. Evaluation of clinical outcome

After completing SRT, chest x-ray films and serial chest CT scans were checked for all cases to evaluate treatment outcomes at 2, 4, 6, 9, 12, 18, and 24 months after completion. Routine blood test results were also examined in all cases at the same time. Lactate dehydrogenase (LDH) and serum Krebs von den Lungen-6 (KL-6) were also collected at the same time as a serum marker of RP. The local tumor response was evaluated using the Response Evaluation Criteria in Solid Tumors Group [15]. Tumor response was assessed by follow-up chest radiography and CT scan. In accordance with WHO criteria, tumor response was defined as complete if all abnormalities that were anatomically related to the tumor disappeared after treatment, and defined as partial if the maximum size of these abnormalities decreased by ≧ 50%. Toxicities were evaluated using the National Cancer Institute-Common Toxicity Criteria (NCI-CTC) version 3.0. The toxicity data was collected retrospectively from the patient files. The following grading system was assigned to the RP: Grade 1, asymptomatic (radiographic findings only); Grade 2, symptomatic and not interfering with activities of daily living (ADL); Grade 3, symptomatic and interfering with ADL or O_2 indicated; Grade 4, life-threatening (ventilatory support indicated), and Grade 5, death.

Maximum dose, minimum dose, D95, field size, and homogeneity index (HI) were evaluated (Table 2). HI was defined as the ratio of maximum dose to minimum dose. In our institution, HI must be below 1.40 in order to keep the dose within the PTV more homogeneous. In analyzing the dose to the lung, the V_5-V_{20}, MLD, and conformity index (CI) were evaluated (Table 2). V_5-V_{50} and MLD was calculated for both lungs. The lung volume minus the PTV (PTV excluded) was used as the volume of lung parenchyma. In this study, CI was defined as the ratio of treated volume (TV) (the definition of TV was the volume covered by minimum dose within PTV) to PTV (i.e. CI = TV/PTV) according to JCOG0403 protocol, although this concept might be old and be used hardly. This definition of the CI is the opposite comparing with the CI defined by Knoos *et al.* (CI = PTV/TV) [16]. The higher the CI values obtained indicated that the areas irradiated were less conformal. Three patients had lesions located in the hilar/central tumor region according to Timmerman *et al.* [10].

2.4. Statistical analysis

CI and MLD between RP positive and negative were compared using an unpaired multiple *t*-tests. Statistical significant was defined as p value of <0.05.

Table 2: DVH characteristics in treatment planning.

No.	Tumor location	Isocenter Dose	BED_{10} (Gy)	Beam	Co-pulanar	Collimators (mm)	Field size (mm^2)	V_{20} (%)	V_{40} (%)	V_{45} (%)	MLD (cGy)	D95 (cGy)	HI (%)	CI (%)
1	peripheral	48Gy/4f	105.6	6	2	67 × 74	4958	5.0	2.0	1.0	206	4408	126	171
2	peripheral	48Gy/4f	105.6	6	2	40 × 61	2440	5.0	2.0	1.0	488	4547	128	219
3	peripheral	48Gy/4f	105.6	6	2	30 × 31	930	1.0	0.5	0.3	172	4462	120	202
4	peripheral	48Gy/4f	105.6	6	2	60 × 46	2760	7.0	3.0	2.0	445	4325	128	147
5	peripheral	48Gy/4f	105.6	6	2	48 × 63	3024	3.0	2.0	1.0	298	4443	117	157
6	peripheral	48Gy/4f	105.6	6	2	67 × 67	4489	8.0	3.0	1.0	406	4435	123	197
7	peripheral	48Gy/4f	105.6	6	2	49 × 57	2793	8.0	2.0	1.0	510	4432	118	187
8	peripheral	48Gy/4f	105.6	6	2	45 × 51	2295	3.0	1.0	0.5	259	4468	125	182
9	peripheral	48Gy/4f	105.6	6	2	55 × 60	3300	7.0	2.0	1.0	404	4515	118	168
10	peripheral	48Gy/4f	105.6	6	2	59 × 68	4012	9.0	2.0	1.0	573	4511	122	170
11	peripheral	48Gy/4f	105.6	6	2	69 × 68	4692	7.0	2.9	2.0	404	4380	126	204
12	peripheral	48Gy/4f	105.6	7	2	79 × 97	7663	9.0	6.1	5.2	579	4355	134	169
13	rt perihilar/central	48Gy/4f	105.6	6	2	51 × 51	2601	7.0	2.7	1.9	585	4633	112	322
	lt perihilar/central	48Gy/4f	105.6	6	2	49 × 57	2793	6.0	2.6	1.9	353	4629	110	257
14	perihilar/central	48Gy/8f	76.8	6	2	45 × 63	2835	7.0	1.0	0.5	568	4557	124	184
15	peripheral	48Gy/4f	105.6	6	2	40 × 42	1680	5.0	2.0	1.0	313	4617	109	282
16	peripheral	48Gy/4f	105.6	6	2	70 × 54	3780	10.0	5.0	3.0	791	4500	126	173
17	peripheral	48Gy/4f	105.6	6	2	48 × 62	2976	6.0	1.0	0.5	426	4405	121	310
18	peripheral	48Gy/4f	105.6	6	2	55 × 53	2915	4.0	1.0	0.5	291	4780	115	148
19	perihilar/central	48Gy/6f	86.4	6	2	59 × 59	3481	11.0	3.0	1.0	541	4835	139	170
20	peripheral	48Gy/4f	105.6	7	4	49 × 46	2254	11.0	1.0	0.5	321	4851	112	164
21	peripheral	48Gy/4f	105.6	6	2	50 × 56	2800	6.0	1.0	0.5	426	4602	118	192
22	peripheral	48Gy/4f	105.6	6	2	55 × 57	3135	7.0	2.0	1.0	440	4890	119	175
23	peripheral	48Gy/4f	105.6	7	4	60 × 58	3480	8.0	2.0	1.0	422	4585	112	130
24	peripheral	48Gy/4f	105.6	6	2	35 × 34	1190	2.0	0	0	230	4468	117	173
25	peripheral	48Gy/4f	105.6	6	2	32 × 40	1280	4.0	0.5	0	353	4591	107	153

BED: biologically effective doses, CI: conformity index, f: fractions, HI: homogeneity index, MLD: mean lung dose, Vx: irradiated lung volume more than × Gy

3. Results

The patients ranged in age from 50 to 84 years with a median of 77 years (73.8 ± 8.6 years). Female to male ratio was 4:21. The volumes irradiated over 5, 7, 10, 13, 15, 20, 30, 35, 40, 45, 50 Gy were designated as V_5, V_7, V_{10}, V_{13}, V_{15}, V_{20}, V_{30}, V_{35}, V_{40}, V_{45}, V_{50} respectively. Nine patients had chronic lung disorders, and four were in a postoperative state. Four patients had emphysema, three had interstitial pneumonia (IP), and one had chronic obstructive pulmonary disease (COPD). The length of follow-up ranged from 10 to 28 months with a median of 17 months (16.1 ± 7.1 months). During the follow-up period, only two tumors showed local regrowth in the meaning of local control (Table 3). The overall radiation treatment-time was five or 6 days in all cases excluding a single patient and the single patient was 8 days. The absolute volumes for every patient: ITV, PTV, the volume enclosed by the 48Gy total-isodose, the 24Gy-isodose-volume were shown in Table 4.

Seven out of the 25 patients suffered from RP of grade 2 or more in the NCI-CTC version 3.0. All patients with RP had a cough, continuous fevers, severe dyspnea, and showed infiltrative changes in both irradiated and non-irradiated areas on chest CT (Figures 1 and 2). Three patients out of 25 treated with SRT died from a fatal RP. There were seven patients: one had RP at 2 months, one at 3 months, one at 9 months, two at 5 months, and two at 6 months. In all of the seven patients, pneumonitis spread out beyond the PTV. The overall incidence rate of RP grade 2 or more determined by the Kaplan-Meier method was 29.2% at 18 months after completing SRT (Figure 3). Various clinical as well as therapeutic factors were analyzed for their possible relationships to the incidence of RP (Table 2). There were no significant relations between the incidence of RP and with or without co-morbidity lung disease (χ^2 test: $p = 0.9400$). Only two cases (22%) developed RP out of nine patients with co-morbidity lung disease. In all of the 25 patients, LDH levels remained normal during the follow-up period. Three of the seven patients with RP had high values of serum KL-6 before SRT, and the other four had normal serum KL-6 level. Additionally, RP had been observed in three patients who had high levels of serum KL-6 before SRT.

The high value of CI showed a significant correlation with the occurrence of RP, while MLD (Figure 4), field size, PTV volume, and V5, V7, V10, V13, and V15 (p value according to unpaired t-test was 0.1966, 0.1658, 0.2351, 0.3831, and 0.3963, respectively) showed no correlations with RP. Additionally, V20, V30, V35, V40, V45, and V50 showed no significant correlations with the incidence of RP, either (p value was 0.6768, 0.8369, 0.8318, 0.8044, 0.7544, and 0.9218, respectively) (Figure 5). Even when the volumes V5-V50 were given in absolute units (cm3) for the lung parenchyma (PTV excluded), there were no significant

Table 3: Treatment results and RP grading

No.	Follow up (Months)	Dead or alive (cause of death)	Local control	Control out of field	RP grading
1	16	dead (primary)	PD	PD	G0
2	19	dead (aging)	PR	control	G0
3	20	alive	PR	PD	G1
4	19	alive	PR	control	G1
5	19	alive	CR	control	G1
6	16	alive	PD	PD	G1
7	15	alive	CR	control	G1
8	10	dead (primary)	PR	control	G0
9	14	alive	CR	control	G0
10	4	dead (aging)	PR	control	G0
11	10	alive	PR	control	G2 (2Mo)
12	11	alive	PR	control	G1
13	4	dead (RP)	CR	control	G5 (3Mo)
14	11	alive	CR	control	G2 (5Mo)
15	10	alive	PR	control	G1
16	7	dead (RP)	CR	PD	G5 (6Mo)
17	9	alive	CR	control	G3 (6Mo)
18	9	alive	CR	control	G4 (9Mo)
19	9	alive	PR	control	G1
20	8	dead (primary)	CR	control	G1
21	8	alive	CR	control	G0
22	6	dead (RP)	CR	control	G5 (5Mo)
23	7	alive	PR	control	G1
24	3	alive	PR	control	G0
25	2	alive	NE	NE	G0

CR: complete response, NE: not evaluate, PD: progressive disease, PR: partial response, RP: radiation pneumonitis, SD: stable disease

correlations between V5–V50 and the incidence of RP (Table 5). The patients with RP had a mean CI of 222–66%, while the mean for patients without RP was 180–33% ($p = 0.0394$) (Figure 6). There was no significant correlation between both the ITV and PTV volume and the incidence of RP ($p = 0.7415$ and $p = 0.7675$, respectively).

CI showed no significant correlations with V5-V20 and MLD. CI correlated significantly with the ITV (both t-test and $\chi 2$ test: $p < 0.0001$).

No patient had NCI-CTC Grade 3 or 4 toxicities such as fatigue, dermatitis associated with radiation, dysphagia, esophagitis, and pain in chest wall.

4. Discussion

Although extracranial stereotactic irradiation is an emerging treatment modality utilized by an increasing number of institutions in this field [1-4], only a few institutions have published their clinical results. SRT is accepted as a treatment method in medically inoperable non-small cell lung cancer or in patients who refused surgery. Promising results have been reported for this treatment method, with high local control rates and low incidence of complications [7,17-21]. A multi-institutional prospective trial (JCOG 0403) is currently in progress in Japan. This paper describes the experience of treating 25 patients with small (< 4 cm) lung tumors with four fractions of 12Gy. An unusually high rate of severe (grade 3 or more) RP (20%) and mortality (12%) was noticed and we are searching for reasons to explain these results, because we notice that these rates are far beyond other reported series. In this study, since the clinical data is collected retrospectively, the data is biased and there is a lack of information. Especially the lung function data of 11 patients (44%) are missing.

In our study, some of the patients started to suffer from "pneumonitis" almost 12 months after radiotherapy. These patients suffered from lung fibrosis plus pneumonia. RP is generally seen within 3 months of radiation and, in contrast, radiation fibrosis, which is thought to represent scar/fibrotic lung tissue, is usually a "late effect" seen >3 months after radiation. These may be difficult to distinguish from each other. RP is a sub-acute (weeks to months from treatment) inflammation of the end bronchioles and alveoli. The clinical picture may be very similar to acute bacterial pneumonia with fatigue, fever, shortness of breath, non-productive cough, and a pulmonary infiltrate on chest x-ray. The infiltrate on chest x-ray should include the area treated to high dose, but may

Table 4: The absolute volumes for every patient: ITV, PTV, the volume enclosed by the 48Gy total-isodose, the 24Gy-isodose-volume

Case	ITV (cm^3)	PTV (cm^3)	V48 (cm^3)	V24 (cm^3)
1	13.9	66.8	54.4	284
2	10.1	40.1	25.9	108
3	1.0	7.5	0.0	30
4	9.6	34.9	6.7	141
5	11.4	45.2	0.3	85
6	34.2	85.1	22.8	166
7	17.2	51.0	3.0	135
8	9.7	33.7	10.5	57
9	16.4	54.4	8.1	175
10	30.8	81.9	25.3	258
11	30.0	79.1	37.5	212
12	126.9	239.4	98.4	263
13 rt	5.0	20.5	16.5	123
lt	6.4	26.4	15.6	114
14	15.5	47.5	20.1	147
15	5.0	10.2	3.4	109
16	49.9	120.9	46.7	303
17	5.1	29.4	6.4	128
18	13.2	42.5	0.6	247
19	36.2	85.0	6.8	238
20	8.4	29.0	2.1	81
21	9.0	29.6	1.7	103
22	18.5	56.5	1.7	119
23	17.3	50.8	1.8	153
24	1.8	10.6	2.6	39
25	1.7	10.5	0.4	36

extend outside of these regions. The infiltrates may be characteristically "geometric" corresponding to the radiation portal, but may also be ill defined.

CI may be a useful DVH factor for predicting the occurrence of RP after SRT for lung tumors. Although the CI was first proposed in 1993 by the Radiation Therapy Oncology Group (RTOG) and described in Report 62 of the International Commission on Radiation Units and Measurements (ICRU), it has not been included in routine practice [16,22-25]. The CI is a measure of how well the volume of a radiosurgical dose distribution conforms to the size and shape of a target volume, and is a complementary tool for scoring a given plan or for evaluating different treatment plans for the same patient. The radiation CI gives a consistent method for quantifying the degree of conformity based on iso-dose surfaces and volumes. Care during interpretation of radiation CI must always be taken, since small changes in the minimum dose can dramatically change the treated volume [16]. With the growth of conformal radiotherapy, the CI may play an important role in the future. However, this role has not yet been defined, probably because the value of conformal radiotherapy is just beginning to be demonstrated in terms of prevention of adverse effects and tumor control [26-29]. In our study, there was a significant association between CI with RP rate ($p = 0.0394$). A higher CI is less conformal. Figure 6 appears to say that the CI should be less than 2.00 since the most patients (15/18 cases) without RP were covered. This is a reflection of the number of beams and the spreading out of the prescribed dose. It is recommended that efforts be directed to reduce CI (= TV/PTV) in treatment planning. For that purpose, the minimum irradiation dose within PTV should be raised to reduce the TV. CI is generally used as a criterion to evaluate treatment plan. It has no relation with the volume of

Table 5: The correlation comparing the occurrence of RP with V5-V50

		V5	V7	V10	V13	V15	V20	V30	V35	V40	V45	V50
p	value RP	0.2500	0.2422	0.3208	0.2742	0.2717	0.4063	0.5858	0.7557	0.8220	0.9307	0.4780
	with	744 ± 134	631 ± 117	495 ± 95	368 ± 70	307 ± 56	210 ± 39	124 ± 24	96 ± 18	75 ± 15	48 ± 11	1 ± 1
	without	604 ± 52	504 ± 47	400 ± 43	290 ± 32	244 ± 26	174 ± 20	108 ± 14	88 ± 13	70 ± 11	47 ± 9	4 ± 2

mean ± SD (cm^3)

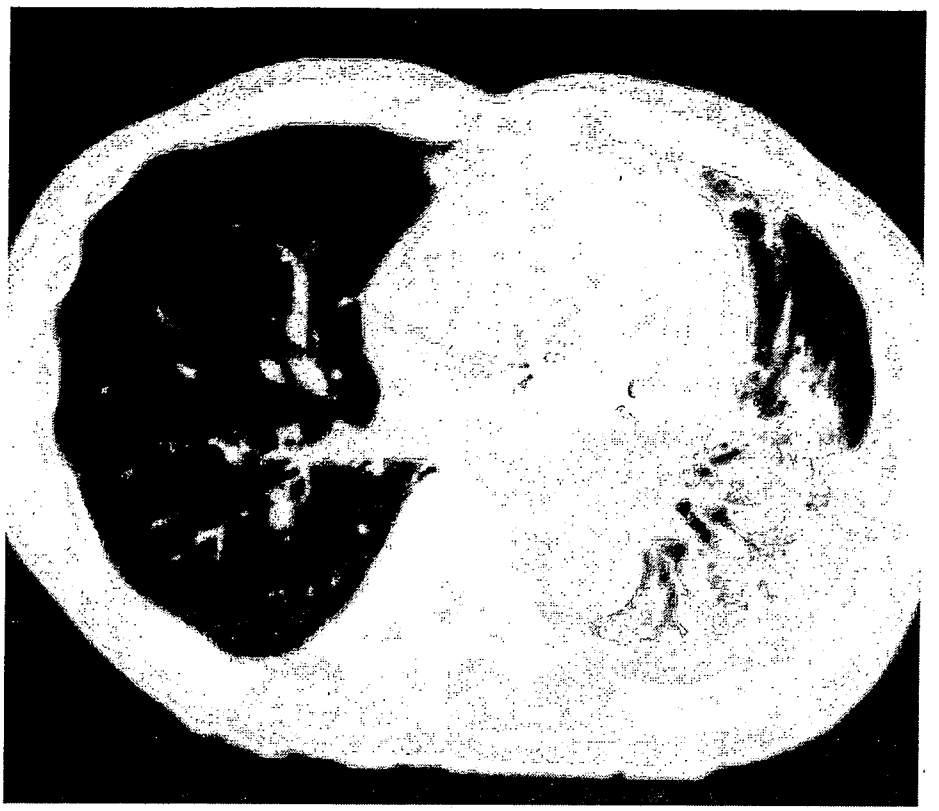

Figure 1
Computed tomography (CT) image of radiation pneumonitis (RP) (patient No. 11).

the irradiated lung. From a radiotherapeutic/-biological point of view, it is not likely that CI has a true predictive value for development of RP. CI is related to volume receiving very high radiation dose (90 % of prescribed dose). Lung tissue is vulnerable even to low dose. Therefore parameters related to volumes receiving low doses (i.e. V_{10} or MLD) are much more likely to correlate with toxicity. As the cases numbers were small, the co-relationship of CI and PR possibly may be coincident.

In our study, statistical analysis did not show significant association between MLD and RP rate, which were different from results of lung toxicity from conventional fractionation [11,30,31]. In our study, CI had no significant correlation with MLD. MLD was not a useful factor for predicting the occurrence of RP. V_5 rather than V_7, V_{10}, V_{13}, V_{15}, and V_{20} had the strongest correlation with MLD, although in our study neither V_5 nor MLD was a useful factor for predicting RP.

In a similar study by Paludan *et al.* [32] reporting dose-volume related parameters in a similar number of patients (N = 28), no relationship between DVH parameters and changes in dyspnea was found. They found that deterioration of lung function was more likely related to the patient co-morbidity (COPD) than to dose-volume related parameters. However, in the present analysis, there were no significant relations between the incidence of RP and with or without co-morbidity lung diseases.

The levels of KL-6 [17,33-35] and LDH are reported to be sensitive markers of RP, but in our study, both markers were not very sensitive. A few patients undergoing single high-dose SRT suffered from radiation pneumonitis,

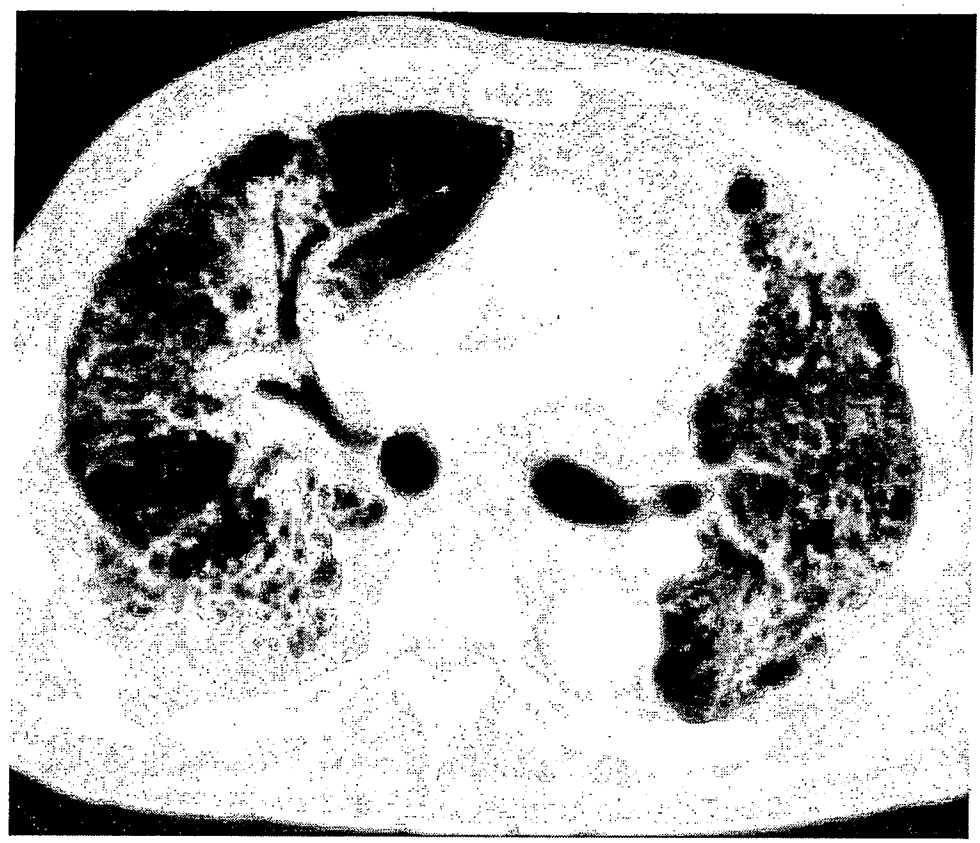

Figure 2
CT image of RP (patient No. 13).

which was treated by administration of steroids. It is known that intense radiation changes and fibrosis without symptoms (Grade 1) will be found in the majority of patients after hypo-fractionated SRT. In addition, pneumonias develop regularly in these medically inoperable patients, and the combination of these can easily mislead to a diagnosis of RP. Misclassification in such a small number of patients will lead to a huge overestimation of the real incidence. In particular the fact that some of the patients already suffered from IP may have obscured the occurrence of RP. E.g. Figure 2 is at "best" a patient suffering from bronchiolitis obliterans with organizing pneumonia (BOOP), with the bilateral infiltrates.

It is debatable whether V_{20} can be applied to SRT in the same way as it is applied to conventional radiotherapy [11,36]. Our >20 Gy irradiated volume of the whole lung was 1.0–9.0% (average 4.83%), which was markedly smaller than that reported by Graham *et al.* [11]. In a previous study using whole-body irradiation, Wara *et al.* [37] demonstrated that eight Gy is the tolerance dose in the lung in single fractional irradiation. V_{20} was defined for standard fractionation. Biologically equivalent dose (BED) would be about 6.7 Gy ($\alpha/\beta = 3$) with 12 Gy per fractionation. Thus, V_5 and V_7 would be important factor.

Many studies [7,18-20,38] have reported no patients who showed RP of Grade 3 or more in lung SRT. Additionally, only low incident rate of grade 2 RP (2.4% [20], 3% [21], 5.4% [18], and 7.2% [39]) was reported. Hara *et al.* [17] at the International Medical Center of Japan reported that 3 of the 16 patients (19%) experienced RP of Grade 3 severity with SRT of 20–35 Gy in a single fraction. Belderbos *et al.* [39] suggested additional reductions of the security margins for PTV definition and introduction of inhomogeneous dose distributions within the PTV. Com-

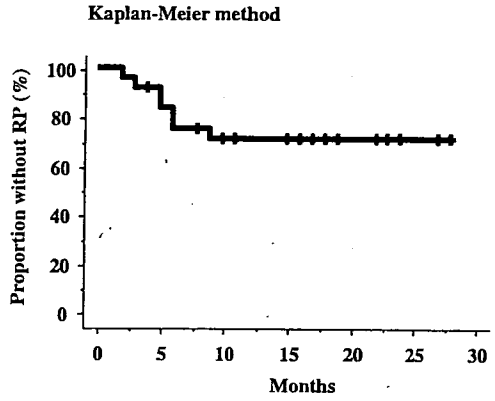

Figure 3
Kaplan-Meier plot of time from treatment until RP grade2 to 5. There were seven patients: one had RP at 2 months, one at 3 months, one at 9 months, two at 5 months, and two at 6 months.

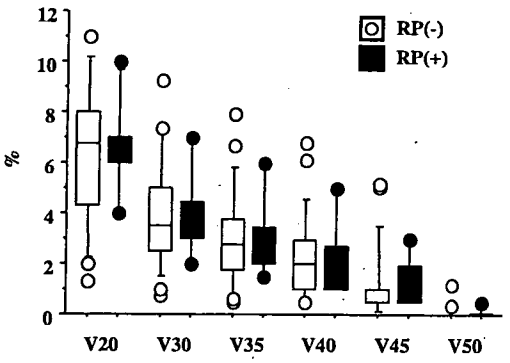

Figure 5
The correlation comparing the occurrence of RP grade 2 or more with V_{20}-V_{50}.

pared with these reports, the occurrence rate of RP was much higher in our institution. As for its cause, we submit that many patients in our study had poor respiratory function, many patients were judged as inoperable because of IP, and some cases had recurrent lung tumors after surgery. If the relative gantry angles and the number of beams were arranged more properly, the CI ratio would be made lower, since their factors probably are directly related to the CI. Additionally it is essential to use small fields. We set the leaves at 5 mm outside the PTV in order to make the dose distribution within the PTV more homogeneous. This may be the reason why we got so unacceptably high CI. We might have had to set the leaves at the margin of the PTV according to the ongoing Radiation Therapy Oncology Group protocols. There must be something wrong with either the way targets are irradiated. Clinical target volume including spicula formation (= ITV) + 5 mm ITV-PTV margin + 5 mm PTV-leaf margins might have been unnecessary large margins. However, our PTV (53.4 ± 47.0 cm^3, median: 43.8 cm^3) was almost equal to the PTV reported by Fritz *et al.* [38] (median: 45.0 cm^3) without any symptomatic RP. It appears that in this study large volumes of lung parenchyma were irradiated to such high

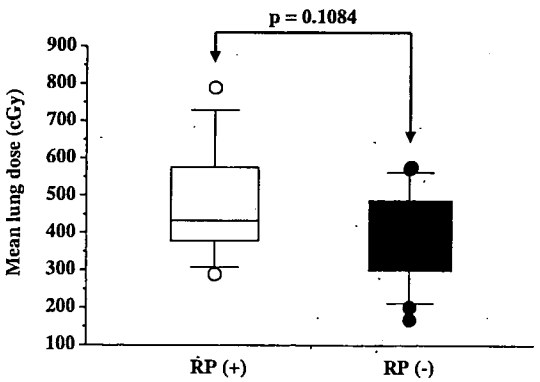

Figure 4
The correlation comparing the occurrence of RP grade 2 or more with MLD.

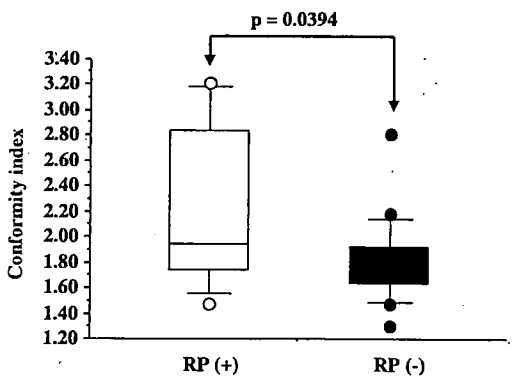

Figure 6
The correlation comparing the occurrence of RP grade 2 or more with CI.

doses as the minimum dose within planning target volume (= high the TV and high CI value), which may explain the high incidence of lung toxicity.

Timmerman *et al.* [10] recently published a paper reporting of a high incidence of RP after SRT. They found an unacceptable high rate, if the tumor was located more centrally. In our study, this tendency was not seen (only one out of patients with severe RP had a central tumor).

Hope *et al.* [40] found that RP is correlated to the volume of the high dose region. These data (the value of CI and the incidence of RP had the strongest correlation) may support another hypothesis that RP probably has associations with high dose regions rather than with low dose regions (V_5-V_{20}). However, in our study, V_{30}, V_{35}, V_{40}, V_{45}, and V_{50} showed no significant correlations with the incidence of RP, either. It may be no wonder that the CI does not show a relation with V_{30}-V_{50}, because the V_{30}-V_{50} depends on the absolute volume of the PTV, not on the CI. Only the treatment technique will show such correlation.

The use of multiple non-coplanar static ports achieved homogeneous target dose distributions and avoided high doses to normal tissues, despite the limitation of the beam arrangement from the use of the body frame and couch structure.

5. Conclusion

In our institution, exceptionally high incidence of Grade 3–5 radiation pneumonitis after SRT for lung tumors was seen. Even in SRT, when large volumes of lung parenchyma are irradiated to such high doses as the minimum dose within planning target volume, the incidence of lung toxicity can become high. Further observations of the radiation changes in the lung after SRT are needed.

Competing interests

The author(s) declare that they have no competing interests.

Authors' contributions

• HY conducted follow-up examinations and contributed to data analysis and drafting the manuscript.

• KN oversaw the administration of radiation therapy to the patients, conducted follow-up.

• NN oversaw the administration of radiation therapy to the patients, conducted follow-up.

• HK contributed to data analysis and drafting the manuscript.

• MT oversaw the administration of radiation therapy to the patients, conducted follow-up.

• IH performed assessments of patients.

• KS performed assessments of patients.

• NS performed assessments of patients.

• KO contributed to drafting the manuscript.

All authors read and approved the final manuscript.

References

1. Nagata Y, Negoro Y, Aoki T, Mizowaki T, Takayama K, Kokubo M, Araki N, Mitsumori M, Sasai K, Shibamoto Y, Koga S, Yano S, Hiraoka M: **Clinical outcomes of 3D conformal hypofractionated single high-dose radiotherapy for one or two lung tumors using a stereotactic body frame.** *Int J Radiat Oncol Biol Phys* 2002, **52:**1041-1046.
2. Uematsu M, Shioda A, Tahara K, Fukui T, Yamamoto F, Tsumatori G, Ozeki Y, Aoki T, Watanabe M, Kusano S: **Focal, high dose, and fractionated modified stereotactic radiation therapy for lung carcinoma patients a preliminary experience.** *Cancer* 1998, **82:**1062-1070.
3. Nakagawa K, Aoki Y, Tago M, Terahara A, Ohtomo K: **Megavoltage CT-assisted stereotactic radiosurgery for thoracic tumors original research in the treatment of thoracic neoplasms.** *Int J Radiat Oncol Biol Phys* 2000, **48:**449-457.
4. Wulf J, Hadinger U, Oppitz U, Thiele W, Ness-Dourdoumas R, Flentje M: **Stereotactic radiotherapy of targets in the lung and liver.** *Strahlenther Onkol* 2001, **177:**645-655.
5. Hara R, Itami J, Kondo T, Aruga T, Abe Y, Ito M, Fuse M, Shinohara D, Nagaoka T, Kobiki T: **Stereotactic single high dose irradiation of lung tumors under respiratory gating.** *Radiother Oncol* 2002, **63:**159-163.
6. Onimaru R, Shirato H, Shimizu S, Kitamura K, Xu B, Fukumoto S, Chang TC, Fujita K, Oita M, Miyasaka K, Nishimura M, Dosaka-Akita H: **Tolerance of organs at risk in small-volume, hypofractionated, image-guided radiotherapy for primary and metastatic lung cancers.** *Int J Radiat Oncol Biol Phys* 2003, **56:**126-135.
7. Hof H, Herfarth KK, Munter M, Hoess A, Motsch J, Wannenmacher M, Debus J: **Stereotactic single-dose radiotherapy of stage I non-small-cell lung cancer (NSCLC).** *Int J Radiat Oncol Biol Phys* 2003, **56:**335-341.
8. Whyte RI, Crownover R, Murphy MJ, Martin DP, Rice TW, DeCamp MM Jr, Rodebaugh R, Weinhous MS, Le QT: **Stereotactic radiosurgery for lung tumors preliminary report of a phase I trial.** *Ann Thorac Surg* 2003, **75:**1097-1101.
9. Takai Y, Mituya M, Nemoto K, Ogawa Y, Kakuto Y, Matusita H, Takeda K, Takahashi C, Yamada S: **[Simple method of stereotactic radiotherapy without stereotactic body frame for extracranial tumors].** *Nippon Igaku Hoshasen Gakkai Zasshi* 2001, **61:**403-407.
10. Timmerman R, McGarry R, Yiannoutsos C, Papiez L, Tudor K, DeLuca J, Ewing M, Abdulrahman R, DesRosiers C, Williams M, Fletcher J: **Excessive toxicity when treating central tumors in a phase II study of stereotactic body radiation therapy for medically inoperable early-stage lung cancer.** *J Clin Oncol* 2006, **24:**4833-4839.
11. Graham MV, Purdy JA, Emami B, Harms W, Bosch W, Lockett MA, Perez CA: **Clinical dose-volume histogram analysis for pneumonitis after 3D treatment for non-small cell lung cancer (NSCLC).** *Int J Radiat Oncol Biol Phys* 1999, **45:**323-329.
12. Matsuo Y, Takayama K, Nagata Y, Kunieda E, Tateoka K, Ishizuka N, Mizowaki T, Norihisa Y, Sakamoto M, Narita Y, Ishikura S, Hiraoka M: **Interinstitutional variations in planning for stereotactic body radiation therapy for lung cancer.** *Int J Radiat Oncol Biol Phys* 2007, **68:**416-425.
13. Lagerwaard FJ, Van Sornsen de Koste JR, Nijssen-Visser MR, Schuchhard-Schipper RH, Oei SS, Munne A, Senan S: **Multiple "slow" CT**

scans for incorporating lung tumor mobility in radiotherapy planning. *Int J Radiat Oncol Biol Phys* 2001, **51**:932-937.
14. van Sornsen de Koste JR, Lagerwaard FJ, Schuchhard-Schipper RH, Nijssen-Visser MR, Voet PW, Oei SS, Senan S: **Dosimetric consequences of tumor mobility in radiotherapy of stage I non-small cell lung cancer--an analysis of data generated using 'slow' CT scans.** *Radiother Oncol* 2001, **61**:93-99.
15. Therasse P, Arbuck SG, Eisenhauer EA, Wanders J, Kaplan RS, Rubinstein L, Verweij J, Van Glabbeke M, van Oosterom AT, Christian MC, Gwyther SG: **New guidelines to evaluate the response to treatment in solid tumors. European Organization for Research and Treatment of Cancer, National Cancer Institute of the United States, National Cancer Institute of Canada.** *J Natl Cancer Inst* 2000, **92**:205-216.
16. Knoos T, Kristensen I, Nilsson P: **Volumetric and dosimetric evaluation of radiation treatment plans: radiation conformity index.** *Int J Radiat Oncol Biol Phys* 1998, **42**:1169-1176.
17. Hara R, Itami J, Komiyama T, Katoh D, Kondo T: **Serum levels of KL-6 for predicting the occurrence of radiation pneumonitis after stereotactic radiotherapy for lung tumors.** *Chest* 2004, **125**:340-344.
18. Takayama K, Nagata Y, Negoro Y, Mizowaki T, Sakamoto T, Sakamoto M, Aoki T, Yano S, Koga S, Hiraoka M: **Treatment planning of stereotactic radiotherapy for solitary lung tumor.** *Int J Radiat Oncol Biol Phys* 2005, **61**:1565-1571.
19. Song DY, Benedict SH, Cardinale RM, Chung TD, Chang MG, Schmidt-Ullrich RK: **Stereotactic body radiation therapy of lung tumors: preliminary experience using normal tissue complication probability-based dose limits.** *Am J Clin Oncol* 2005, **28**:591-596.
20. Onishi H, Nagata Y, Shirato H, Gomi K, Karasawa K, Arimoto T, Hayakawa K, Takai Y, Kimura T, Takeda A: **Stereotactic hypofractionated high-dose irradiation for stage I non-small cell lung carcinoma: Clinical outcomes in 273 cases of a Japanese multi-institutional study.** *ASCO* 2004, **22(14S)**:. (July 15 Supplement) abstract No: 7003
21. Wulf J, Haedinger U, Oppitz U, Thiele W, Mueller G, Flentje M: **Stereotactic radiotherapy for primary lung cancer and pulmonary metastases: a noninvasive treatment approach in medically inoperable patients.** *Int J Radiat Oncol Biol Phys* 2004, **60**:186-196.
22. Anonymous: **Prescribing, recording and reporting photon beam therapy (supplement to ICRU Report 50).** In *Report 62, International Commission on Radiation Units and Measurements* Washington, DC; 1999.
23. Shaw E, Kline R, Gillin M, Souhami L, Hirschfeld A, Dinapoli R, Martin L: **Radiation Therapy Oncology Group: Radiosurgery quality assurance guidelines.** *Int J Radiat Oncol Biol Phys* 1993, **27**:1231-1239.
24. Feuvret L, Noel G, Mazeron JJ, Bey P: **Conformity index: a review.** *Int J Radiat Oncol Biol Phys* 2006, **64**:333-342.
25. Paddick I: **A simple scoring ratio to index the conformity of radiosurgical treatment plans. Technical note.** *J Neurosurg* 2000, **93(Suppl 3)**:219-222.
26. Takayama K, Nagata Y, Negoro Y, Mizowaki T, Sakamoto T, Sakamoto M, Aoki T, Yano S, Koga S, Hiraoka M: **Treatment planning of stereotactic radiotherapy for solitary lung tumor.** *Int J Radiat Oncol Biol Phys* 2005, **61**:1565-1571.
27. Armstrong J, McGibney C: **The impact of three-dimensional radiation on the treatment of non-small cell lung cancer.** *Radiother Oncol* 2000, **56**:157-167.
28. Dearnaley DP, Khoo VS, Norman AR, Meyer L, Nahum A, Tait D, Yarnold J, Horwich A: **Comparison of radiation side-effects of conformal and conventional radiotherapy in prostate cancer: A randomised trial.** *Lancet* 1999, **353**:267-272.
29. Lee WR, Hanks GE, Hanlon AL, Schultheiss TE, Hunt MA: **Lateral rectal shielding reduces late rectal morbidity following high dose three-dimensional conformal radiation therapy for clinically localized prostate cancer: Further evidence for a significant dose effect.** *Int J Radiat Oncol Biol Phys* 1996, **35**:251-257.
30. Yorke ED, Jackson A, Rosenzweig KE, Merrick SA, Gabrys D, Venkatraman ES, Burman CM, Leibel SA, Ling CC: **Dose-volume factors contributing to the incidence of radiation pneumonitis in non-small cell lung cancer patients treated with three-dimensional conformal radiation therapy.** *Int J Radiat Oncol Biol Phys* 2002, **54**:329-339.
31. Hernando ML, Marks LB, Bentel GC, Zhou SM, Hollis D, Das SK, Fan M, Munley MT, Shafman TD, Anscher MS, Lind PA: **Radiation induced pulmonary toxicity: a dose-volume histogram analysis in 201 patients with lung cancer.** *Int J Radiat Oncol Biol Phys* 2001, **51**:650-659.
32. Paludan M, Traberg Hansen A, Petersen J, Grau C, Hoyer M: **Aggravation of dyspnea in stage I non-small cell lung cancer patients following stereotactic body radiotherapy: Is there a dose-volume dependency?** *Acta Oncol* 2006, **45**:818-822.
33. Kohno N, Hamada H, Fujioka S, Hiwada K, Yamakido M, Akiyama M: **Circulating Antigen KL-6 and Lactate Dehydorogenase for Monitoring Irradiated Patients with Lung Cancer.** *Chest* 1992, **102**:117-122.
34. Kohno N, Kyoizumi S, Awaya Y, Fukuhara H, Yamakido M, Akiyama M: **New serum indicator of interstitial pneumonitis activity: sialylated carbohydrate antigen KL-6.** *Chest* 1989, **96**:68-73.
35. Goto K, Kodama T, Sekine I, Kakinuma R, Kubota K, Hojo F, Matsumoto T, Ohmatsu H, Ikeda H, Ando M, Nishiwaki Y: **Serum levels of KL-6 are useful biomarkers for severe radiation pneumonitis.** *Lung Cancer* 2001, **34**:141-148.
36. Kohno N, Kyoizumi S, Awaya Y, Fukuhara H, Yamakido M, Akiyama M: **New serum indicator of interstitial pneumonitis activity: sialylated carbohydrate antigen KL-6.** *Chest* 1989, **96**:68-73.
37. Wara WM, Phillips TL, Margolis LW, Smith V: **Radiation pneumonitis: A new approach to the derivation of time-dose factors.** *Cancer* 1973, **32**:547-552.
38. Fritz P, Kraus HJ, Muhlnickel W, Hammer U, Dolken W, Engel-Riedel W, Chemaissani A, Stoelben E: **Stereotactic, single-dose irradiation of stage I non-small cell lung cancer and lung metastases.** *Radiat Oncol* 2006, **1**:30.
39. Belderbos JS, De Jaeger K, Heemsbergen WD, Seppenwoolde Y, Baas P, Boersma LJ, Lebesque JV: **First results of a phase I/II dose escalation trial in non-small cell lung cancer using three-dimensional conformal radiotherapy.** *Radiother Oncol* 2003, **66**:119-126.
40. Hope AJ, Lindsay PE, El Naqa I, Alaly JR, Vicic M, Bradley JD, Deasy JO: **Modeling radiation pneumonitis risk with clinical, dosimetric, and spatial parameters.** *Int J Radiat Oncol Biol Phys* 2006, **65**:112-124.

J. Radiat. Res., 49, 55–62 (2008)

Regular Paper

Pathological Changes in the Gastrointestinal Tract of a Heavily Radiation-exposed Worker at the Tokai-mura Criticality Accident

Hiroshi IGAKI[1], Keiichi NAKAGAWA[1]*, Hiroshi UOZAKI[2], Masaaki AKAHANE[1], Yoshio HOSOI[1,3], Masashi FUKAYAMA[2], Kiyoshi MIYAGAWA[3], Makoto AKASHI[4], Kuni OHTOMO[1] and Kazuhiko MAEKAWA[5]

Acute radiation exposure/Criticality accident/Multiple organ dysfunction syndrome/Gastrointestinal syndrome.

Gastrointestinal syndrome after high-dose acute radiation whole body exposure is difficult to treat, although it is a well-known complication. In this report, we describe the clinical and pathological features of a patient who died after the criticality accident which occurred in Japan on 30 September 1999. The patient was estimated to have been exposed to 16–25 Gy equivalent of gamma ray, and died of multiple organ failure after acute radiation syndrome, especially gastrointestinal syndrome, on day 82. The stomach and small intestine contained a large amount of blood clots and the gastrointestinal epithelial cells were almost totally depleted at autopsy. In addition, the degree of the mucosal damage was dependent on the segment of the gastrointestinal tract; the mucosa of stomach, ileum and ascending colon was entirely depleted, but the esophagus, descending and sigmoid colon and rectum retained a small portion of the epithelial cells. From the posture of the patient at the time of exposure, the absorbed dose was presumed to be highest in the right-anterior abdomen. This agreed with the pathological differences in the mucosal damage by the position in the abdomen, which depended presumably on the radiation dose. This is the first report documenting the relationship between the absorbed dose and the severity of gastrointestinal damages *in vivo*.

INTRODUCTION

Patients suffering from accidental acute radiation exposure are often difficult to treat for several reasons: the difficulty and uncertainty of estimating the exposure dose, the heterogeneity of the absorbed dose in the body, the scarcity of medical staff who are well acquainted and experienced with the treatment of radiation damage to the organs, and the lack of sufficient human data on acute radiation damage to the organs after a single high-dose radiation exposure.[1)]

Recent studies have revealed the close relationship between acute radiation syndrome and multiple organ dysfunction syndrome (MODS) or multiple organ failure (MOF).[2,3)] Moreover, the gastrointestinal tract plays an important role in developing MODS by the collapse of the intestinal barrier function from enteric bacterium after radiation exposure as well as after severe burns or other trauma.[3,4)]

The criticality accident occurred at the uranium fuel processing facility of JCO Co. Ltd. in Tokai-mura, Ibaraki, Japan in 1999. Two workers were pouring uranyl nitrate solution manually from a bucket into a precipitation tank, when the tank reached the critical state. Three workers received mixed gamma ray and neutron beam. Two of the victims died due to radiation damage. In this report, we focused on the gastrointestinal syndrome of the patient who was exposed most heavily and was treated at our hospital. We present the clinical course and pathological findings related to the irradiation damage in the patient's gastrointestinal tract.

MATERIALS AND METHODS

Clinical course of the patient

The patient was 35-year-old male. The patient's exposure was estimated to be a systemic mean dose of 16–25 Gy equivalent of gamma ray by the criticality accident at JCO

*Corresponding author: Phone: +81-3-5800-8666,
Fax: +81-3-5800-8935,
E-mail: nakagawa-rad@umin.ac.jp
Departments of [1]Radiology, [2]Pathology, and [3]Radiation Biology, University of Tokyo Hospital, Tokyo, Japan; [4]Division of Radiation Health, National Institute of Radiological Sciences, Chiba, Japan; [5]Kanto Central Hospital, Tokyo, Japan.
doi:10.1269/jrr.07058